ORIGINAL ARTICLE

bioTROPICA   ASSOCIATION FOR TROPICAL BIOLOGY AND CONSERVATION   WILEY

The mechanical stability of the world's tallest broadleaf trees

Tobias D. Jackson[1,2] (iD) | Alexander F. Shenkin[2] | Noreen Majalap[3] | Jamiluddin Bin Jami[4] | Azlin Bin Sailim[4] | Glen Reynolds[4] | David A. Coomes[1] | Chris J. Chandler[5] | Doreen S. Boyd[5] | Andy Burt[6] | Phil Wilkes[6,7] | Mathias Disney[6,7] | Yadvinder Malhi[2]

[1]Forest Ecology and Conservation Group, Department of Plant Sciences, University of Cambridge, Cambridge, UK

[2]Environmental Change Institute, School of Geography and the Environment, University of Oxford, Oxford, UK

[3]Phytochemistry Unit, Forest Research Centre, Sabah, Malaysia

[4]South East Asia Rainforest Research Partnership (SEARRP), Sabah, Malaysia

[5]School of Geography, University of Nottingham, Nottingham, UK

[6]Department of Geography, University College London, London, UK

[7]NERC National Centre for Earth Observation (NCEO), Leicester, UK

Correspondence
Tobias D. Jackson, Forest Ecology and Conservation Group, Department of Plant Sciences, University of Cambridge, CB2 3EA, UK.
Email: tobydjackson@gmail.com

Abstract

The factors that limit the maximum height of trees, whether ecophysiological or mechanical, are the subject of longstanding debate. Here, we examine the role of mechanical stability in limiting tree height and focus on trees from the tallest tropical forests on Earth, in Sabah, Malaysian Borneo, including the recently discovered tallest tropical tree, a 100.8 m *Shorea faguetiana* named Menara. We use terrestrial laser scans, in situ strain gauge data and finite element simulations, to map the architecture of tall tropical trees and monitor their response to wind loading. We demonstrate that a tree's risk of breaking due to gravity or self-weight decreases with tree height and is much more strongly affected by tree architecture than by material properties. In contrast, wind damage risk increases with tree height despite the larger diameters of tall trees, resulting in a U-shaped curve of mechanical risk with tree height. Our results suggest that the relative rarity of extreme wind speeds in north Borneo may be the reason it is home to the tallest trees in the tropics.

Abstract in MALAY is available with online material.

KEYWORDS

biomechanics, Danum Valley, gravitational stability, maximum tree height, Menara, terrestrial laser scanning (TLS), wind damage

1 | INTRODUCTION

Tall trees are an essential store of carbon and an inspiration to the public and to ecologists alike (Lindenmayer & Laurance, 2016, Bastin et al. 2018, Lutz et al. 2018). Recently, the world's tallest tropical tree, a 100.8 m *Shorea faguetiana* (named "Menara"), has been discovered in Sabah, Malaysian Borneo (Shenkin et al., 2019). Trees over 80 m tall have long been recognized in temperate regions—notably

the conifer *Sequoia sempervirens* in California and the broadleaf *Eucalyptus regnans* in Tasmania, but the discovery of such tall trees in the tropics is recent. Record-sized tropical trees have also recently been discovered in Africa ($H \sim 81.5$ m, Hemp et al., 2017) and South America ($H \sim 88.5$ m, Gorgens et al., 2019).

Tree height growth is driven by the intense competition for light in young forest stands (MacFarlane & Kane, 2017) but why emergent trees continue to grow upwards once they have escaped competition, and what determines the mean and maximum height of forest canopies, is less well understood. Why do the world's tallest broadleaf trees grow to about 100 m in height, and not 50 m or 500 m? Possible answers to this question are that tree height is limited by mechanics, hydraulics, or carbohydrate supply. The relative importance of these limiting factors will likely vary according to local climate, and the tallest broadleaf trees are likely to be found in regions with little seasonal water stress, such as aseasonal tropical (Moles et al., 2009a, Klein et al. 2015).

The hydraulic limitation theory posits that the negative water potentials in the vascular systems at the tops of trees, driven by gravity and by demand outstripping supply around midday, inhibit the transfer of water from the vascular system into the cytoplasm of plants (Koch, Stillet, Jennings, & Davis, 2004, Ishii et al. 2014). This effect, and the increased risk of embolism, is predicted to lead to lower tree heights in drier regions and is supported by the correlation between canopy height and water availability at the global scale (Moles et al., 2009b, Klein et al. 2015). The carbohydrate transport theory posits that it is the ability of leaves to supply carbohydrates to distant tissues against resistance that limits tree to around 100 m (Jensen & Zwieniecki, 2013) and explains the relationship between water availability and tree height as being determined by climate constraints on leaf size.

The mechanical limitation theory, which is the subject of the current paper, suggests that tree height is limited by either gravity or wind damage risk. King, Davies, Tan, and Nur Supardi (2009) showed that understory trees can approach their gravitational limits (i.e., approach the Euler buckling limit), but that the increased diameter to height ratios in canopy trees leads to a high gravitational safety margin. The fact that canopy and emergent trees are exposed to increased wind loading (for a review see Moore, Gardiner, & Sellier, 2018) suggests that wind dominates the mechanical limitation of taller trees, but this has not been confirmed by measurements. Trees are known to adjust their growth pattern to their local wind environment (Bonnesoeur, Constant, Moulia, & Fournier, 2016; Telewski, 2006) but whether the increased diameter to height ratios in canopy trees is sufficient to compensate for the increased wind exposure remains an open question.

In addition to the three mechanisms above, Domec et al. (2008) suggested that the wind-induced bending of the tree stem may negatively affect water transport thus limiting tree height through a combination of the mechanical and hydraulic mechanisms. Also, recent work has highlighted the role of lightning as a potential driver of large tree mortality (Yanoviak et al., 2020).

This study presents initial findings on both aspects of the mechanical limitation hypothesis in the context of the tallest tropical forests on earth, in northern Borneo. Our key questions are as follows:

1. *How does gravitational stability vary with tree height, architecture, and material properties?* Recent progress in terrestrial laser scanning (TLS) techniques allow us to estimate the volume of the crowns of tall trees without allometric equations. We use this to test the relative importance of variations in crown size and material properties in terms of their effects on gravitational stability.
2. *How does the risk of wind damage change with tree height?* Taller trees are exposed to higher wind speeds, but they also have better resistance to bending due to their higher trunk diameter and modulus of elasticity (see Table Table 1 for glossary). We measure the bending strains produced in the tree trunk under wind loading for a small sample of tall trees to explicitly test whether these effects balance out.
3. *Is Menara, the world's tallest tropical tree, close to its mechanical limits?* We use finite element analysis to explore combined effects of gravity and wind on Menara.

2 | METHODS

2.1 | Description of field sites

The island of Borneo is host to the world's tallest tropical forests. Danum Valley is situated in the state of Sabah, Malaysia (4°57'N 117°48'E) and is home to a permanent 50 ha forest monitoring plot (Reynolds, Payne, Sinun, Mosigil, & Walsh, 2011). Within this plot, all the trees with dbh ≥ 1 cm have been tagged and measured and identified to species level where possible. Our strain gauge study site is located within a 1 ha intense monitoring plot containing 450 trees ≥ 10 cm dbh with a basal area of 32 m^2, 178 known species, and 50 trees whose species are not yet determined (Riutta et al., 2018). Tree height and crown dimensions have also been estimated using a laser rangefinder (Sullivan et al., 2018). The Belian plot in the Maliau Basin Conservation Area (4°44'N 116°58'E), also in Sabah, is a permanent sample plot with trees ≥ 10 cm dbh monitored. It has a basal area of 41.5 m^2, 135 known species, 4 species determined to genus, and 5 individuals of undetermined taxonomy.

2.2 | Terrestrial laser scanning and tree architecture

TLS data were collected in Danum Valley during April 2017 and in Maliau in July 2018 using a Riegl VZ-400 (for protocols see Wilkes et al., 2017). In this study, we focussed on 16 trees from Danum Valley and 5 trees from Maliau, in addition to Menara (Table 2). We manually extracted trees from the plot level point cloud and

TABLE 1 Glossary of key terms

Term	Definition
Gravitational max height, H_{max}	The tallest a tree can grow without collapsing under gravity
Modulus of elasticity, E	A measure of a material's resistance to bending
K	The ratio of crown weight to trunk weight
Bending strain	Extension per unit length—in this case along a tree trunk
Wind–strain gradient	The slope of the best fit line relating bending strain to squared wind speed
Risk factor, R	The measured height of the tree divided by the maximum height consistent with safety, either from wind or gravity

trimmed the individual tree point clouds manually (Figure S3) using specifically designed software (Vicari, 2017). We used a specifically designed cylinder fitting algorithm (*TreeQSM*; Åkerblom, 2017) to fit 360 quantitative structure models (QSMs) to each tree-level point cloud, varying the fitting parameters. The most plausible resulting QSM was selected manually by comparing it to the point cloud (see Appendix S2). This process is subjective, and all of the point clouds and QSMs are available online. TLS scanning and data processing for Menara followed a similar protocol, except that drone imagery of the crown was used to supplement the TLS data coverage using structure-from-motion techniques (Shenkin et al., 2019). For this tree, the QSM of the stem was manually defined using a vertical profile of trunk diameter measurements taken directly from the point cloud. Buttresses were removed from the tree-level point clouds prior to cylinder fitting to generate the QSMs and a cylinder of the same height as the buttress attached to the bottom of the QSM after fitting. The resolution of the point clouds decreased with tree height due to occlusion and the divergence of the TLS laser beam. Therefore, the cylinder fitting process cannot detect the small branches at the tops of the trees and the QSMs systematically underestimated tree height (Figure S2). We therefore use height measurements taken from the point clouds for all analyses except for Menara, which was directly measured by climbing (Figure 1).

As noted by Osunkoya et al., (2007), no generalizable definition of branching order or the bottom of the crown is available in the literature. We therefore manually defined the point at which the crown starts for each QSM (Figure S3). We then calculated the ratio of crown mass to stem mass, K, and the positions of the centers of mass for the crown and for the whole tree (Figure S3). Previous work in similar forests found that variation in crown architecture was primarily intraspecific, with only a small proportion of the total variance explained by species (Iida et al., 2011; Osunkoya et al., 2007). These studies also reported a decrease in relative crown size with tree height, which was fit with a power law function (Osunkoya et al., 2007). Therefore, in order to generalize the risk factor calculation, we fit a power law relationship $K = 6.92H^{-0.69}$ to the data using the Matlab curve fitting toolbox (Mathworks, 2017). This same relationship was used for all trees in Figure 2b so that comparisons between continents or across material properties gradients are not affected by it. The intercept and exact shape of the risk factors depend on the details of this relationship, but the negative trend,

difference between continents and effect of material properties do not (Appendix S5). It would be interesting to test for systematic variability in this parameter using a larger data set.

2.3 | Gravitational stability

The most relevant material properties for mechanical stability are the green wood density, ρ_{gw}, modulus of elasticity, E_{gw}, and modulus of rupture, MOR_{gw}. We collated material properties data from the literature, mainly from Niklas and Spatz (2010), see Appendix S1 for further details of the sources and Table 2 for the values used in the analysis.

We then calculated the theoretical maximum height each tree could reach before collapsing under gravity, H_{max}, using two different models. The "classical" model (Equation 1) of a tapering beam with a circular cross-section (Greenhill, 1881) and the "top-weight" model which includes a top-weight to represent the crown centered at $0.9H$ (King & Loucks, 1978). Mathematically, the only difference between the two models is the value of the constant, C. In the top-weight model, the weight of the crown is included as per equation 2 which depends on the parameter K, the ratio between stem and crown mass. In the classical model, we chose $C = 1.7464$, so that the two models converge when the top weight is set to 0.

$$H_{max} = C \left(E_{gw} D_0^2 / 4\rho_{gw} \right)^{1/3} \tag{1}$$

$$C = \left(\frac{0.334K^2 + 0.08655K + 0.007601}{0.6125K^3 + 0.1695K^2 + 0.02907K + 0.001427} \right)^{1/3} \tag{2}$$

where D_0 is the diameter at the base of the tree, we use the diameter at breast height since these measurements are readily available and already adjusted for the presence of buttresses.

2.4 | Wind–strain data collection and processing

Since there is no tower near this plot, anemometers were attached to tall trees (trees 1 and 6) boomed out from the stem. Cup anemometers were mounted at 25 m and 35 m on tree 1 (Figure S3). In the case

TABLE 2 Overview of the trees in this study, botanical authors given after species names. TLS ID can be used to identify the point cloud and QSM for each tree in the online materials. ρ_{gw} is the green wood density, E_{gw} is the green wood modulus of elasticity, and MOR_{gw} is the green wood modulus of rupture

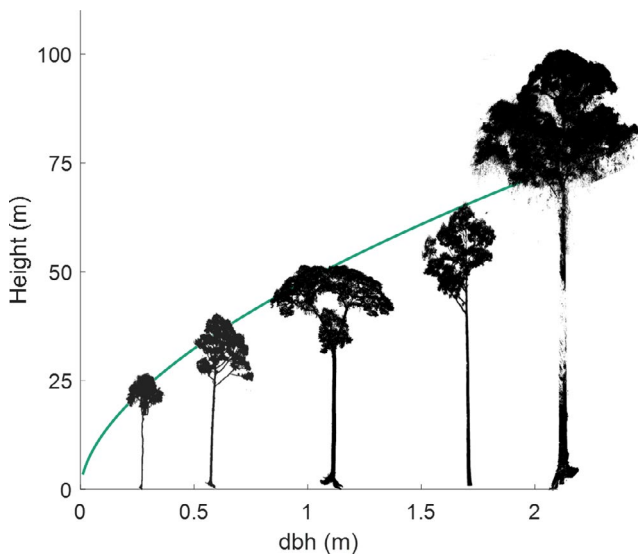| #	Site	Tree tag	TLS ID	Genus & species. Botanical author	DBH cm	Height m	ρ_{gw} kgm^{-3}	E_{gw} MNm^{-2}	MOR_{gw} MNm^{-2}
1	DV	30,343	A1	Parashorea malaanonan. (Blanco) Merr	110	51	641	9,100	61
2	DV	30,296	B2	Chisocheton. Blume	29.8	23	626	7,443	53
3	DV	30,281	C3	Pometia pinnata. J.R.Forst. & G.Forst.	32.2	28	787	9,399	69
4	DV	30,313	D4	Shorea parvifolia. Wyatt-Sm. ex P.S.Ashton	55	39	513	6,700	48
5	DV	30,476	E5	Aporusa benthamiana. Hook	23.3	24	781	9,326	68
6	DV	10,498	F6	Shorea parvifolia	73	46	513	6,700	48
7	DV	10,542	G7	Terminalia citrina. (Gaertn.) Roxb. ex Flem	49.2	42	961	13,000	94
8	DV	20,447	H8	Parashorea malaanonan	100	56	641	9,100	61
9	DV	20,445	-	Orophea myriantha. Merr	20.6	17	747	9,680	70
10	DV	20,419	I10	Not identified	39.4	31	747	9,680	70
11	DV	30,409	J11	Caryodaphnopsis tonkinensis. Airy Shaw	43.5	39	747	9,680	70
12	DV	10,676	K12	Shorea pauciflora. King	24.1	34	689	9,700	68
13	DV	20,523	L13	Syzygium panzer. R.Br. ex Gaertn	40.2	33	798	9,531	70
14	DV	10,612	-	Diospyros tuberculata. Bakh	35.3	34	567	6,728	47
15	DV	20,557	M15	Canarium pilosum. A.W.Benn	29.9	32	593	6,200	41
16	DV	20,596	-	Not identified	21.1	27	747	9,680	70
17	DV	20,593	N17	Eusideroxylon zwageri. Teijsm. & Binn	73.3	43	1,282	17,700	143
18	DV	10,643	-	Orophea myriantha	18.6	18	747	9,680	70
19	DV	20,649	-	Eusideroxylon zwageri	35.4	22	1,282	17,700	143
20	DV	50,214	O20	Parashorea malaanonan	115.0	52	641	9,100	61
21	DV	20,629	P23	Shorea johorensis. Foxw	135.0	53	689	9,700	68
22	DV	Menara	-	Shorea faguetiana. Heim	2.13	100.8	673	9,700	66
23	MLA	102	MLA_157	Shorea gibbosa. Brandis	171.2	69.2	625	9,000	67
24	MLA	60	MLA_215	Shorea faguetiana	162.9	59.2	673	9,700	66
25	MLA	152	MLA_38	Shorea dasyphylla. Foxw	110.2	46.7	609	9,700	63
26	MLA	158	MLA_39	Payena microphylla. (de Vriese) Burck	92.7	43.9	700	9,356	67
27	MLA	195	MLA_40	Shorea parvifolia	157.8	57.3	513	6,700	48

of tree 6, a cup anemometer was mounted at 19 m and a 2D sonic anemometer at 30 m. The cup anemometers were Vector Instruments A100LK/5M and recorded wind speeds at 0.1 Hz, and the 2D sonic anemometer was a Gill Sonic 1, recording at 1 Hz. This arrangement means that our wind data are site-specific and cannot be translated to the standard 10 m above canopy height point of measurement. However, we found that this unusual method proved highly useful with no substantial changes in the results whichever of the four anemometers data were used for the analysis (see Appendix S6). In order to measure the tree's bending in response to wind, we attached pairs of strain gauges to the stems of 19 trees at approximately 1.3 m.

We used three Campbell Scientific CR1000 data loggers and two CR23X data loggers to record the bending strain data from October 2016 until April 2017. For the seven trees logged with CR1000 data loggers, we collected hundreds of hours of data and found a clear bending strain signal (Figure 2a). We also found clear signals for 9 of the 12 trees monitored with CR23X data loggers, although the data availability was lower and the data were noisier. This complicated the uncertainty analysis and the error propagation for the combined wind–strain gradient against tree height model.

The raw data consist of two mV readings per tree at 4 Hz, and we calculated a single maximum strain signal for each tree. This process

involved (1) multiplying the raw strain signal by calibration coefficients to transform from units of mV to strain; (2) bandpass filtering the data to smooth out drift (3) re-projecting the signals onto into the North and East facing directions; and (4) combining each pair of strain signals into a single maximum strain signal. We calculated the modal maximum bending strain (Wellpott 2008) and absolute maximum wind speed for each aggregation period (10 min or 1 min). Using the maxima negates the need for a gust factor (Gardiner, Peltola, & Kellomäki, 2000) and focuses on the bending strains most relevant to wind damage. We then regressed maximum wind against


FIGURE 1 Tree height against trunk diameter (dbh) based on the continental allometric equation for Asia (Feldpausch et al. 2011). Images of trees from this study, derived from terrestrial laser scanning data, are overlaid for context. Menara, the world's tallest tropical tree is at the far right

maximum strain and calculated the gradient. This approach accounts for the dynamic nature of wind loading, but does not explicitly account for the dynamic nature of tree motion. Hale, Gardiner, Wellpott, Nicoll, and Achim (2012) used a similar approach and Schindler and Mohr (2018) recently demonstrated that the dynamic components of tree motion were unimportant in their study site. We conducted some exploratory analysis (not shown) and found a similarly low importance of dynamic effects in our data. The obvious caveat here is that dynamic effects may become important at the higher wind speeds most relevant to wind damage. The wind speed measurement system proved useful and wind–strain gradients did not vary much whichever anemometer they were derived from (see Appendix S6 and S7).

2.5 | Risk factor calculations

We calculated risk factors in order to compare the roles of wind and gravity in maximum height limitation. The gravitational risk factors were defined as the ratio of the measured height (based on the point clouds since the QSMs systematically under-estimate tree height) to the modeled maximum height, $R_{grav} = H/H_{max}$. We generalized gravitational risk factors using the continental height-diameter allometries (Feldpausch et al. 2011) and, in the case of the top-weight model, the power law relationship between K and H described above. We also used data on the systematic variation in material properties between tall and short trees reported by Jagels, Eq uiza, Maguire, and Cirelli (2018) to estimate its effect on gravitational stability.

In order to calculate wind damage risk factors, we extrapolated from field data to estimate what the bending strain would be at a chosen threshold wind speed e.g. 20 ms^{-1}, ε_{20}. The risk factor is then $R_{wind} = \varepsilon_{20}/\varepsilon_{break}$, where ε_{break} is the breaking strain (Appendix
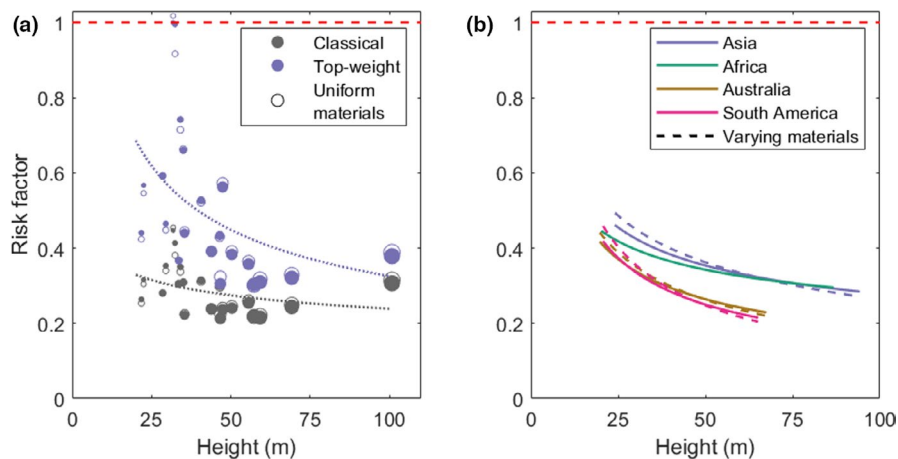
FIGURE 2 (a) Gravitational risk factors for trees in this study calculated using the classical model and top-weight model. The hollow markers represent the risk factor calculations using the mean material properties of all trees, and the solid markers represent species-specific material properties. Fit lines were calculated based on the latter. (b) Gravitational risk factors of trees based on the continental height-diameter allometries using the top-weight model. Solid lines represent uniform material properties while dashed lines indicate material properties varying with height as reported by (Jagels et al., 2018). The red dashed lines at risk factor = 1 shows the point at which a tree would be expected to buckle under its own weight

S1). These risk factors are necessarily relative to the chosen wind speed as well as the point of measurement and aggregating window length. We therefore focus on relative risk factors instead of absolute risk factors. In order to directly compare these results with other sites, we would need data on the return time of extreme wind events and wind measurements from towers approximately 10 m above the canopy. We only considered the risk of trunk snapping and not uprooting in this study, see the limitations section for a discussion of this.

2.6 | Finite element analysis of gravity and wind

Finite element analysis is a numerical method used to calculate the stresses and strains over a complex geometry by splitting the problem up into a large number of finite elements. It has been used to simulate the response of trees to wind loading in conifer forests (Moore & Maguire, 2008) and temperate broadleaf forests (Jackson et al., 2019; Sellier, Fourcaud, & Lac, 2006). We used the QSM of Menara as the input and simulated the effect of increasing wind speed both with and without gravity (for details see Appendix S8). Each cylinder was modeled as a Euler–Bernoulli beam (B31) with the species-specific material properties. A stepwise increasing wind loading was applied to the cylinder model and the deflection of each cylinder was used to re-calculate the wind loading at each time step.

Simulating the effect of gravity proved difficult, since the trees were obviously scanned in the presence of gravity and are therefore pre-stressed structures. The best approximation to a proper treatment of gravity was to apply a reversed gravity force, export the deformed positions of all the branches into a new analysis, then apply a downwards gravity force, and maintain it throughout the simulation. This gave us the desired effect of increasing the moment due to self-weight as the crown deflects under high wind speeds. However, less straight trees failed to stabilize under the downwards gravity load and collapsed, demonstrating that this approach is not generally applicable. This is likely due to the fact that, in nature, trees develop asymmetric material properties to compensate for their asymmetric architecture, but this variation in material properties is extremely difficult to measure and so cannot be included in the simulation.

3 | RESULTS

3.1 | Gravitational risk factors decrease with tree height within a forest canopy

Both the classical and the top-weight models predicted a decrease in gravitational risk factors with tree height (Figure 2a). This means that, as trees get taller, their radial growth is more than sufficient to compensate for their increased weight and height. We also calculated R_{grav} directly from continental height-diameter allometric equations (Feldpausch et al. 2011) and found the same trend (Figure 2b). Comparing continental allometries, we find that trees in Africa and

Asia (the latter data set being dominated by sites in Borneo) have higher R_{grav} than those in South America. The intercept and exact shape of these risk factors depend on the relationship between tree height and K, the ratio of crown weight to stem weight, but the negative trend and difference between continents do not (Appendix S5).

3.2 | Crown size, not material properties, determines gravitational stability

The R_{grav} estimates based on the two models followed a similar pattern (adjusted $R^2 = 0.83$) but the magnitudes diverged substantially between models (Figure 2a). The "top-weight" model predicted that the trees were much closer to their gravitational stability limit than the "classical" model (increase in risk factor ranged from 0.062 to 0.581 with a mean of 0.214). This means that a large, heavy crown substantially increases R_{grav}.

Compared with changes in crown size, material properties (i.e., wood density and modulus of elasticity) had a substantially lower effect on R_{grav}. Differences in risk factors using species-specific or mean material properties ranged from −0.018 to 0.078 with a mean of 0.004. This small effect of materials on R_{grav} is due to the fact that wood density and modulus of elasticity are strongly correlated (Niklas & Spatz, 2010), and it is their ratio that affects R_{grav}. Although its effect on R_{grav} is small, there is a consistent increase in the ratio of wood modulus of elasticity to density with maximum tree height (Jagels et al., 2018). We found that including species-specific material properties (Figure 2a) tended to amplify the difference between short and tall trees, with R_{grav} increasing for shorter trees and decreasing for taller trees. Similarly, Figure 2b used the systematic variation in material properties reported by Jagels et al. (2018) and showed a comparable effect.

3.3 | Wind risk increases with tree height

The second, and more understudied, aspect of mechanical stability is resistance to wind-induced snapping or uprooting (Niklas & Spatz, 2012). As expected, Danum Valley is not a particularly windy site and the maximum recorded wind speed in almost 2000 hr of data collected between August 2016 and March 2017 was a 10 s mean of 7.2 ms^{-1}. The gradient of the wind–strain relationship was steeper for taller trees meaning that taller trees have a higher R_{wind} (Figure 3b). In addition, these results show that variations in material property, such as an increased stiffness for a given density, do not compensate for the increased wind loading.

3.4 | Mechanical risk factor follows a U-shaped curve

Combining the results for R_{grav} and R_{wind}, we show that the resultant mechanical risk profile follows a U-shaped curve with tree
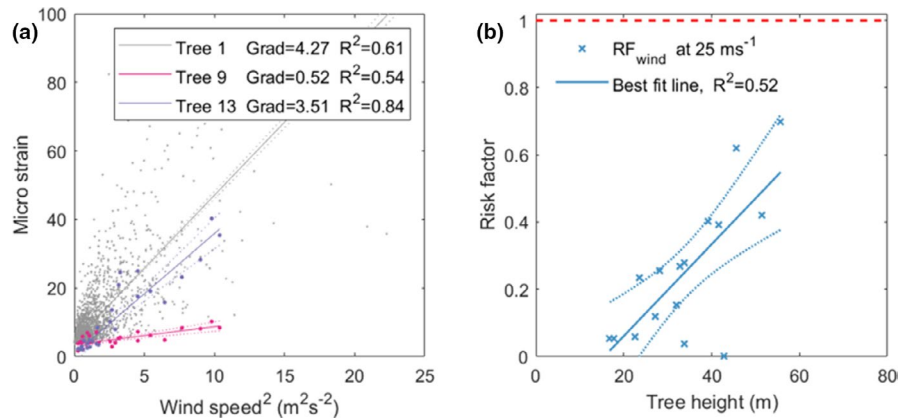
FIGURE 3 (a) 10-min maximum bending strain against maximum squared wind speed measured with the sonic anemometer for three trees. Note the difference in data availability between those logged with CR1000 (tree 1) and CR23X data loggers (trees 9 and 13). (b) Risk factor against tree height assuming a 25 ms⁻¹ wind speed at the position of our sonic anemometer. Individual wind–strain gradients were calculated using a random effects model and a 10-min aggregation period. Risk factors were calculated as the ratio of the predicted strain at 25 ms⁻¹ wind speed to the breaking strain for that species. For details of the fitting process and sensitivity, see Appendix S6 and S7. The red dashed line at risk factor = 1 shows the point at which a tree would be expected to break

height (Figure 4). R_{grav} plays the dominant role in the mechanical stability of small trees, while R_{wind} dominates for tall trees. Figure 4 also demonstrates that the tree height at which this shift takes place depends on the local wind conditions, with wind damage risk dominating earlier in regions which experience more extreme wind-storm events. It should also be noted that the wind and gravitational risk factors are not simply additive, since the gravitational risk factors are derived from a model whereas the wind risk factors are extrapolated from field data which necessarily include gravitational effects.

3.5 | Is Menara, the world's tallest tropical tree, close to its mechanical limits?

The world's tallest tropical tree, Menara, provides an important case study for questions about mechanical stability. Our analysis shows that the greatest mechanical limitation on Menara's height is likely due to wind loading. Extrapolating from our field data to the height of this tree we estimate that it would break at a wind speed of 24.1 ms⁻¹ (measured at the location of the anemometer used in this study). However, this tree, like the previous record holders from Malaysia (Jucker et al., 2018), is situated near the base of a steep valley and will therefore be sheltered from the wind to some degree.

In the above analysis, we consider gravity and wind separately, but in nature they are always combined. In order to simulate the combined effects of wind and gravity, we used finite element analysis based on a TLS-derived beam model of Menara (Figure 5). Our results demonstrate that the effect of wind dominates the bending response of the tree and that the effect of gravity is secondary (Figure 5). The gravity contribution increases with wind speed, since the tree deflection is higher and so the overhanging weight of the crown causes a greater moment. Further finite element simulations were carried out for the other TLS-scanned trees, but complications involving modeling gravity for asymmetric trees without information on the asymmetries in material properties make the results difficult to interpret (see Appendix S8). However, finite element analysis is a promising technique in tree biomechanics (Moore et al., 2018) and could be used in future studies to estimate the strength of buttresses, which are characteristic of these giant trees.
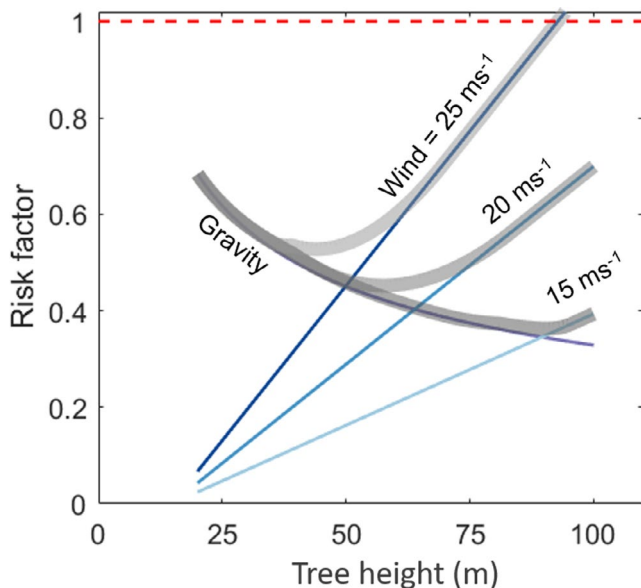
FIGURE 4 U-shaped variation in mechanical risk factor with tree height. The thick gray lines represent overall mechanical risk factors, calculated by interpolating between the gravity and wind lines in the transition region. They do not correspond to the addition of the wind and gravitational risk factors, which would not be appropriate in this case. The red dashed line at risk factor = 1 shows the point at which a tree would be expected to break
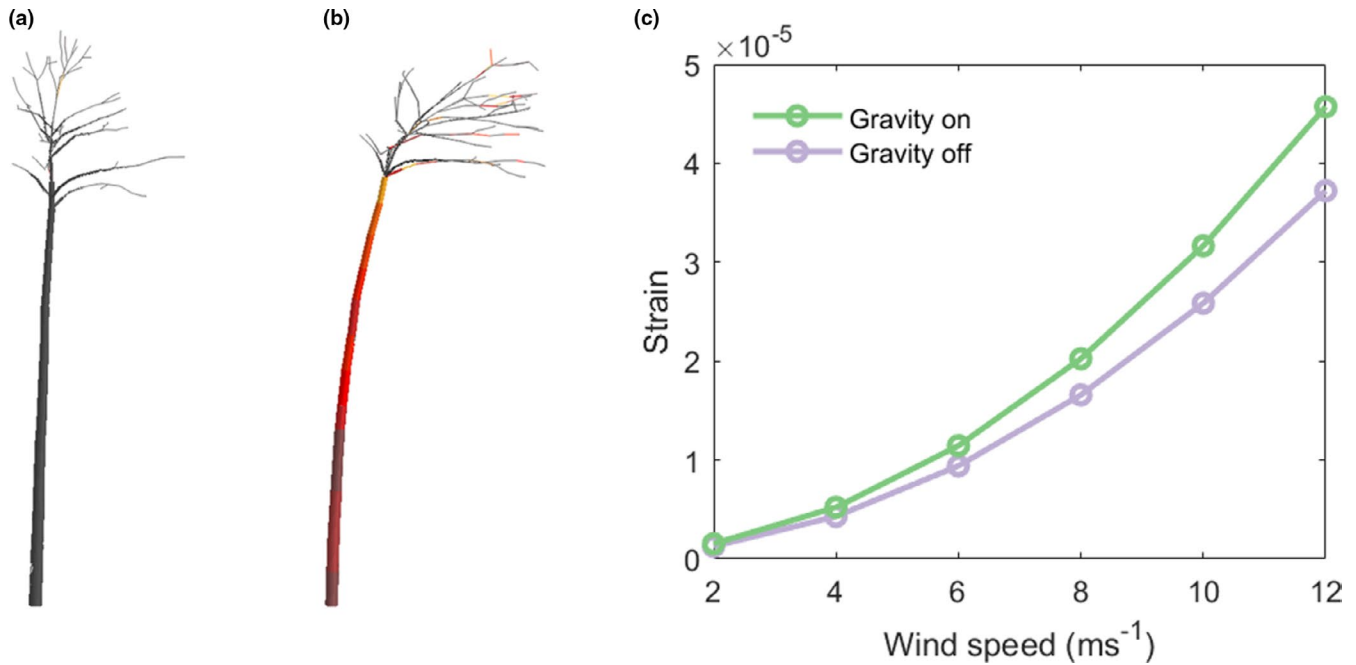
FIGURE 5 (a) Cylinder model of Menara in its rest position. (b) Finite element simulation of the same tree under gravity and 12 ms^{-1} wind loading. (c) Bending strain produced at the base of the stem of the same tree under simulated wind loading with and without gravity

4 | DISCUSSION

We studied the mechanical stability of tall trees in the lowland forests of Sabah, Malaysian Borneo, in order to assess whether these tall trees are subject to mechanical constraints on maximum height. We used TLS data to map the 3D architecture of tall trees and estimated the maximum possible height consistent with gravitational stability. Gravitational risk factors decreased with tree height, meaning that diameter growth more than compensated for increases in tree height, which suggests that this is unlikely to limit tree height. This result supports the hypothesis of King et al. (2009) that understory trees have higher R_{grav} due to the prioritization of vertical height growth under intense competition for light, whereas overstory trees gain less advantage from investing in height growth. We found that accounting for the mass of the tree crown substantially reduced the maximum predicted height and increased the gravitational risk factor, suggesting that many of these trees may be closer to their gravitational limits than previously thought. We also found that material properties had little effect on gravitational stability, emphasizing the importance of tree slenderness and crown size.

Our field measurements show that wind damage risk increases with tree height. This implies that the increased diameter to height ratios of tall trees are not sufficient to compensate for the increased exposure to wind loading. Trees are known to adapt to their local wind environment through increased radial growth (Bonnesoeur et al., 2016; Telewski, 1995), but these measurements suggest that the adaptations are not sufficient in our sample. This is likely because the support costs scale with trunk circumference

and so increase disproportionately with tree height, making it increasingly difficult for a tree to grow radially sufficiently to support the increased wind loading (Givnish, Wong, Stuart-Williams, Holloway-Phillips, & Farquhar, 2014). This suggests that wind loading could provide the limit on tree height in this case, although we would need to conduct extensive measurements and test both the hydraulic and carbohydrate limitation theories in order to be confident of this.

The main limitation of this study is the low sample size, which was determined by the strain sensors and data logging equipment. This study therefore provides preliminary results on an intriguing process, which we hope to confirm in a larger study in time. This limitation does not apply to the gravitational limitation calculations since they are analytical. As with all studies of wind damage in trees, we extrapolate beyond the range of wind speeds observed in our study to calculate the risk factor. This entails the assumption that the wind–tree relationship remains linear and cannot account for the potential effects of streamlining (Vollsinger, Mitchell, Byrne, Novak, & Rudnicki, 2005) or dynamic amplification or damping of tree motion (Ciftci, Brena, Kane, & Arwade, 2013; Spatz, Brüchert, & Pfisterer, 2007). In addition, the finite element analysis did not explicitly include the complex drag forces due to leaves and therefore likely underestimated the wind loading on the crown. Another limitation was that we did not calculate the risk of uprooting, only tree snapping. We do not know of any field technique that can measure the risk of uprooting for large trees in a tropical forest environment. Mode-of-death surveys show a wide variation the relative likelihood of snapping and uprooting (Everham & Brokaw, 1996), presumably driven by site

conditions, and a survey in Danum Valley found that slightly more trees snapped than uprooted in this site (Gale & Hall, 2001). We argue that on average the risk of snapping and uprooting should be similar, as trees are unlikely to have evolved strong mitigation of one risk at the expense of the other (e.g., excessive protection against uprooting would make little sense if tree snapping is the dominant mechanical risk, and *vice versa*). Therefore, we quantified the more tractable risk of snapping and assumed that uprooting is, on average, equally likely.

Overall, the mechanical risk factors follow a U-shaped curve with tree height (Figure 4). The shape of this curve and the point at which mechanical risk shifts from gravity-dominated to wind-dominated depends on the local wind regime. Note that it is the rare extreme wind events (e.g., convective downbursts) that would likely matter, and these rare maximum wind speeds are not necessarily correlated to mean wind speeds. This result suggests that wind plays a role in limiting tree height, which has wide-ranging implications including for forest structure and carbon stocks. Two features of geographical variation of tropical tree height support a role for wind constraints. One is the observation that tree heights in Amazonia and Africa are generally lower than in Borneo (Feldpausch et al. 2011). Northwest Amazonia, in particular, has a wet and aseasonal rainfall regime similar to north Borneo, and hence, little expected seasonal soil water stress (Malhi & Wright, 2004), yet much shorter maximum tree heights. We hypothesize that, compared with the insular climate of Borneo, the continental climates of Amazonia or Central Africa are likely to generate more intense convective events and a higher frequency of extreme winds. Secondly, at a local scale, we note that many of the tallest trees in the Danum Valley area, including Menara, appear to be found in somewhat wind-sheltered regions on the lee side of ridges (Shenkin et al., 2019), again suggesting that maximum winds speeds are a limiting factor. This trend of shorter trees in more wind-exposed areas has also been noted in New Zealand (Coomes, Šafka, Shepherd, Dalponte, & Holdaway, 2018), Dominica (Thomas, Martin, & Mycroft, 2015), and Costa Rica (Lawton, 1982). The general decline of tree height with increasing dry season intensity does suggest that hydraulic or carbohydrate supply is a constraint on maximum height in many tropical forests, but in forests with little seasonal drought our analysis suggest that rare maximum wind speeds may provide the ultimate constraint.

DISCLOSURE STATEMENT
The corresponding author confirms on behalf of all authors that there have been no involvements that might raise the question of bias in the work reported or in the conclusions, implications, or opinions stated.

AUTHOR CONTRIBUTION
TJ, AS, and YM were responsible for the conceptualization and methodology. TJ, NM, JbJ, AbS, GR, AS, AB, PW, and MD were responsible for the investigation, collecting data, and organizing access. AS, JbJ, DC, CC, and DB contributed data on Menara. TJ wrote the original draft, and all authors contributed to its review and editing.

DATA AVAILABILITY STATEMENT
The bending strain and wind speed field data collected for this study are available at the Dryad Digital Repository https://doi.org/10.5061/dryad.v9s4mw6sr and https://doi.org/10.5285/657f420e-f956-4c33-b7d6-98c7a18aa07a. The field data processing scripts, summary data, TLS point clouds, and QSMs (except those for Menara) are all available (https://github.com/TobyDJackson/WindAndTrees_Danum). Point clouds and QSMs for Menara are available at 10.5287/bodleian:KzNpxEOg5. Scripts for calculating tree architectural indices are available in Matlab (https://github.com/TobyDJackson/TreeQSM_Architecture). An updated library for analyzing tree structural information is also available in R (https://github.com/ashenkin/treestruct).

ORCID
Tobias D. Jackson https://orcid.org/0000-0001-8143-6161

REFERENCES
Åkerblom, M. (2017). Inversetampere/Treeqsm: Initial Release. Retrieved from https://zenodo.org/record/844626.

Bastin, J. F., Rutishauser, E., Kellner, J. R., Saatchi, S., Pélissier, R., Hérault, B., ... Zebaze, D. (2018). Pan-tropical prediction of forest structure from the largest trees. *Global Ecology and Biogeography 27*, 1366–1383.

Bonnesoeur, V., Constant, T., Moulia, B., & Fournier, M. (2016). Forest trees filter chronic wind-signals to acclimate to high winds. *New Phytologist*, *210*, 850–860. https://doi.org/10.1111/nph.13836

Ciftci, C., Brena, S. F., Kane, B., & Arwade, S. R. (2013). The effect of crown architecture on dynamic amplification factor of an open-grown sugar maple (*Acer saccharum* L.). *Trees*, *27*, 1175–1189. https://doi.org/10.1007/s00468-013-0867-z

Coomes, D. A., Šafka, D., Shepherd, J., Dalponte, M., & Holdaway, R. (2018). Airborne laser scanning of natural forests in New Zealand

reveals the influences of wind on forest carbon. *Fortiers Ecosystem*, *5*, 10.

Domec, J.-C., Lachenbruch, B., Meinzer, F. C., Woodruff, D. R., Warren, J. M., & McCulloh, K. A. (2008). Maximum height in a conifer is associated with conflicting requirements for xylem design. *Proceedings of the National Academy of Sciences USA*, *105*, –12074. https://doi.org/10.1073/pnas.0710418105

Everham, E. M., & Brokaw, N. V. L. (1996). Forest damage and recovery from catastrophic wind. *Botanical Review*, *62*, 113–185. https://doi.org/10.1007/BF02857920

Feldpausch, T. R., Banin, L., Phillips, O. L., Baker, T. R., Lewis, S. L., Quesada, C. A., ... Lloyd, J. (2011). Height-diameter allometry of tropical forest trees. *Biogeosciences*, *8*, 1081–1106. https://doi.org/10.5194/bg-8-1081-2011

Gale, N., & Hall, P. (2001). Factors determining the modes of tree death in three Bornean rain forests. *Journal of Vegetation Science*, *12*, 337–346. https://doi.org/10.2307/3236847

Gardiner, B., Peltola, H., & Kellomäki, S. (2000). Comparison of two models for predicting the critical wind speeds required to damage coniferous trees. *Ecological Modelling*, *129*, 1–23. https://doi.org/10.1016/S0304-3800(00)00220-9

Givnish, T. J., Wong, S. C., Stuart-Williams, H., Holloway-Phillips, M., & Farquhar, G. D. (2014). Determinants of maximum tree height in *Eucalyptus* species along a rainfall gradient in Victoria, Australia. *Ecology*, *95*, 2991–3007.

Gorgens, E. B., Motta, A. Z., Assis, M., Nunes, M. H., Jackson, T., Coomes, D., ... Ometto, J. P. (2019). The giant trees of the Amazon basin. *Frontiers in Ecology and the Environment*, *17*, 373–374. https://doi.org/10.1002/fee.2085

Greenhill (1881). Determination of the greatest height consistent with stability that a vertical pole or mast can be made, and of the greatest height to which a tree of given proportions can grow. In Proceedings of the Cambridge philosophical society. pp. 65–73

Hale, S. E., Gardiner, B. A., Wellpott, A., Nicoll, B. C., & Achim, A. (2012). Wind loading of trees: Influence of tree size and competition. *European Journal of Forest Research*, *131*, 203–217. https://doi.org/10.1007/s10342-010-0448-2

Hemp, A., Zimmermann, R., Remmele, S., Pommer, U., Berauer, B., Hemp, C., & Fischer, M. (2017). Africa's highest mountain harbours Africa's tallest trees. *Biodiversity and Conservation*, *26*, 103–113. https://doi.org/10.1007/s10531-016-1226-3

Iida, Y., Kohyama, T. S., Kubo, T., Kassim, A. R., Poorter, L., Sterck, F., & Potts, M. D. (2011). Tree architecture and life-history strategies across 200 co-occurring tropical tree species. *Functional Ecology*, *25*, 1260–1268. https://doi.org/10.1111/j.1365-2435.2011.01884.x

Ishii, H. R., Azuma, W., Kuroda, K., & Sillett, S. C. (2014). Pushing the limits to tree height: could foliar water storage compensate for hydraulic constraints in S equoia sempervirens? *Functional Ecology*, *28*(5), 1087–1093.

Jackson, T., Shenkin, A., Kalyan, B., Zionts, J., Calders, K., Origo, N., ... Malhi, Y. (2019). A new architectural perspective on wind damage in a natural forest. *Frontiers in Forests and Global Change*, *1*, 13. https://doi.org/10.3389/ffgc.2018.00013

Jagels, R., Equiza, M. A., Maguire, D. A., & Cirelli, D. (2018). Do tall tree species have higher relative stiffness than shorter species? *American Journal of Botany*, *105*, 1617–1630. https://doi.org/10.1002/ajb2.1171

Jensen, K. H., & Zwieniecki, M. A. (2013). Physical limits to leaf size in tall trees. *Physical Review Letters*, *110*, 018104. https://doi.org/10.1103/PhysRevLett.110.018104

Jucker, T., Asner, G. P., Dalponte, M., Brodrick, P. G., Philipson, C. D., Vaughn, N. R., ... Coomes, D. A. (2018). Estimating aboveground carbon density and its uncertainty in Borneo's structurally complex tropical forests using airborne laser scanning. *Biogeosciences*, *15*(12), 3811–3830. https://doi.org/10.5194/bg-15-3811-2018

King, D. A., Davies, S. J., Tan, S., & Nur Supardi, M. N. (2009). Trees approach gravitational limits to height in tall lowland forests of Malaysia. *Functional Ecology*, *23*, 284–291. https://doi.org/10.1111/j.1365-2435.2008.01514.x

King, D., & Loucks, O. L. (1978). The theory of tree bole and branch form. *Radiation and Environmental Biophysics*, *15*, 141–165. https://doi.org/10.1007/BF01323263

Klein, T., Randin, C., & Körner, C. (2015). Water availability predicts forest canopy height at the global scale A. Mooers (Ed.). *Ecological Letters 18*: 1311–1320.

Koch, G. W., Stillet, S. C., Jennings, G. M., & Davis, S. D. (2004). The limits to tree height. *Nature*, *428*, 851–854. https://doi.org/10.1038/nature02417

Lawton, R. O. (1982). Wind stress and elfin stature in a montane rain forest tree: An adaptive explanation. *American Journal of Botany*, *69*, 1224–1230. https://doi.org/10.1002/j.1537-2197.1982.tb13367.x

Lindenmayer, D. B., & Laurance, W. F. (2016). The Unique Challenges of Conserving Large Old Trees. *Trends in Ecology & Evolution*, *31*, 416–418. https://doi.org/10.1016/j.tree.2016.03.003

Lutz, J. A., Furniss, T. J., Johnson, D. J., Davies, S. J., Allen, D., & Zimmerman, J. K. (2018). Global importance of large-diameter trees. *Global Ecology and Biogeography*, *27*(7), 849–864.

MacFarlane, D. W., & Kane, B. (2017). Neighbour effects on tree architecture: Functional trade-offs balancing crown competitiveness with wind resistance. *Functional Ecology*, *31*, 1624–1636. https://doi.org/10.1111/1365-2435.12865

Malhi, Y., & Wright, J. (2004). Spatial patterns and recent trends in the climate of tropical rainforest regions. *Philosophical Transactions of the Royal Society of London. Series B: Biological Sciences*, *359*(1443), 311–329. https://doi.org/10.1098/rstb.2003.1433.

Mathworks, M. (2017). *MATLAB and Statistics Toolbox Release.* Natick, MA: The MathWorks, Inc.

Moles, A. T., Warton, D. I., Warman, L., Swenson, N. G., Laffan, S. W., Zanne, A. E., ... Leishman, M. R. (2009a). Global patterns in plant height. *Journal of Ecology*, *97*, 923–932. https://doi.org/10.1111/j.1365-2745.2009.01526.x

Moore, J., Gardiner, B., & Sellier, D. (2018). Tree mechanics and wind loading. In A. Geitmann & J. Gril (Eds.), *Plant biomechanics* (pp. 79–106). Cham, Switzerland: Springer International Publishing.

Moore, J. R., & Maguire, D. A. (2008). Simulating the dynamic behavior of Douglas-fir trees under applied loads by the finite element method. *Tree Physiology*, *28*, 75–83. https://doi.org/10.1093/treephys/28.1.75

Niklas, K. J., & Spatz, H. C. (2010). Worldwide correlations of mechanical properties and green wood density. *American Journal of Botany*, *97*, 1587–1594. https://doi.org/10.3732/ajb.1000150

Niklas, K. K. J., & Spatz, H. H.-C. (2012). *Plant physics*. Chicago, IL: University of Chicago Press.

Osunkoya, O. O., Omar-Ali, K., Amit, N., Dayan, J., Daud, D. S., & Sheng, T. K. (2007). Comparative height crown allometry and mechanical design in 22 tree species of Kuala Belalong rainforest, Brunei, Borneo. *American Journal of Botany*, *94*, 1951–1962. https://doi.org/10.3732/ajb.94.12.1951

Reynolds, G., Payne, J., Sinun, W., Mosigil, G., & Walsh, R. P. D. (2011). Changes in forest land use and management in Sabah, Malaysian Borneo, 1990–2010, with a focus on the Danum Valley region. *Philosophical Transactions of the Royal Society B*, *366*, 3168–3176.

Riutta, T., Malhi, Y., Kho, L. K., Marthews, T. R., Huaraca Huasco, W., Khoo, M., ... Ewers, R. M. (2018). Logging disturbance shifts net primary productivity and its allocation in Bornean tropical forests. *Global Change Biology*, *24*, 2913–2928. https://doi.org/10.1111/gcb.14068

Schindler, D., & Mohr, M. (2018). Non-oscillatory response to wind loading dominates movement of Scots pine trees. *Agricultural & Forest*

Meteorology, *250–251*, 209–216. https://doi.org/10.1016/j.agrformet.2017.12.258

Sellier, D., Fourcaud, T., & Lac, P. (2006). A finite element model for investigating effects of aerial architecture on tree oscillations. *Tree Physiology*, *26*, 799–806. https://doi.org/10.1093/treephys/26.6.799

Shenkin, A., Chandler, C. J., Boyd, D. S., Jackson, T., Disney, M., Majalap, N., … Malhi, Y. (2019). The world's tallest tropical tree in three dimensions. *Frontiers in Forests and Global Change*, *2*, 32. https://doi.org/10.3389/ffgc.2019.00032

Spatz, H. C., Brüchert, F., & Pfisterer, J. (2007). Multiple resonance damping or how do trees escape dangerously large oscillations? *American Journal of Botany*, *94*, 1603–1611. https://doi.org/10.3732/ajb.94.10.1603

Sullivan, M. J. P., Lewis, S. L., Hubau, W., Qie, L., Baker, T. R. … Banin, L. F. (2018). Field methods for sampling tree height for tropical forest biomass estimation. *Methods in Ecology and Evolution*, *9*, 1179–1189.

Telewski, F. W. (1995). Wind-induced physiological and developmental responses in trees. *Wind Trees*, *237*, 237–263.

Telewski, F. W. (2006). A unified hypothesis of mechanorperception in plants. *American Journal of Botany*, *93*, 1466–1476.

Thomas, S. C., Martin, A. R., & Mycroft, E. E. (2015). Tropical trees in a wind-exposed island ecosystem: Height-diameter allometry and size at onset of maturity. *Journal of Ecology*, *103*, 594–605. https://doi.org/10.1111/1365-2745.12378

Vicari, M. B. (2017). Leaf separation in TLS data. Retrieved from https://zenodo.org/record/802233#.WlSf_d9l82w.

Vollsinger, S., Mitchell, S. J., Byrne, K. E., Novak, M. D., & Rudnicki, M. (2005). Wind tunnel measurements of crown streamlining and drag relationships for several hardwood species. *Canadian Journal of Forest Research*, *35*, 1238–1249. https://doi.org/10.1139/x05-051

Wellpott, A. (2008). The stability of continuous cover forests. Sch. Geosci. PhD: 160. Retrieved from http://ethos.bl.uk/OrderDetails.do?uin=uk.bl.ethos.663634 .

Wilkes, P., Lau, A., Disney, M., Calders, K., Burt, A., Gonzalez de Tanago, J., … Herold, M. (2017). Data acquisition considerations for Terrestrial Laser Scanning of forest plots. *Remote Sensing of Environment*, *196*, 140–153. https://doi.org/10.1016/j.rse.2017.04.030

Yanoviak, S. P., Gora, E. M., Bitzer, P. M., Burchfield, J. C., Muller-Landau, H. C., Detto, M., … Hubbell, S. P. (2020). Lightning is a major cause of large tree mortality in a lowland neotropical forest. *New Phytologist*, *225*, 1936–1944. https://doi.org/10.1111/nph.16260

SUPPORTING INFORMATION

Additional supporting information may be found online in the Supporting Information section.